This article has been accepted for publication in a future issue of this journal, but has not been fully edited. Content may change prior to final publication. Citation information: DOI 10.1109/TIE.2018.2879293, IEEE Transactions on Industrial Electronics

Geometric Analysis Based Double Closed-loop Iterative Learning Control of Output PDF Shaping of Fiber Length Distribution in Refining Process

Mingjie Li, Ping Zhou, *Senior Member, IEEE*, Hong Wang, *Senior Member, IEEE*, and Tianyou Chai, *Fellow, IEEE*

***Abstract*—In order to improve the pulp quality and to reduce the energy consumption, the fiber length distribution (FLD) is generally employed as one of the important technological indexes in the refining process. Considering that the traditional mean and variance of fiber length are unable to adequately characterize the non-Gaussian distribution properties, this paper proposes a novel geometric analysis based double closed-loop iterative learning control (ILC) method for probability density function (PDF) shaping of output FLD in the refining process. Primarily, a RBF neural network (NN) with Gaussian-type is utilized to approximate the square root PDF in the inner loop, where the RBF basis function parameters (center and width) are tuned between any two adjacent batches by using an ILC law, and the subspace identification method can be applied to establish the state-space model of weight vector. Then, for the sake of accelerating the convergence rate of the closed-loop sysyem, a geometric analysis based ILC method is adopted in the outer loop. Finally, both simulation and experiments demonstrate the effectiveness and practicability of the proposed approach.**

***Index Terms*—Probability density function (PDF), stochastic distribution control (SDC), iterative learning control (ILC), geometric analysis, fiber length distribution (FLD), refining process.**

I. Introduction

As one of the most important parts in the papermaking industry, the refining process mainly supplies pulps meeting certain physical properties for the subsequent papermaking process, whose high energy consumption and low efficiency problems need urgent handling [1]−[3]. The pulp is the final product in the refining process and the principal raw material in the papermaking process, in which the fiber length plays a deterministic role in the pulp quality and paper properties, such as tearing strength, tensile strength, burst strength and so on. As shown in Fig. 1(a), the short fiber will inevitably cause low dewatering rate and high water content, which will greatly increase the energy consumption of paper sheet drying section in papermaking process. In contrast, the long fiber shown in Fig. 1(b) is conducive to the formation of large porosity and the improvement of the dehydration efficiency of paper sheet, reducing the energy consumption in the papermaking process [4]−[9]. However, it also leads to the degradation of paper sheet performances, such as low uniformity and poor quality.

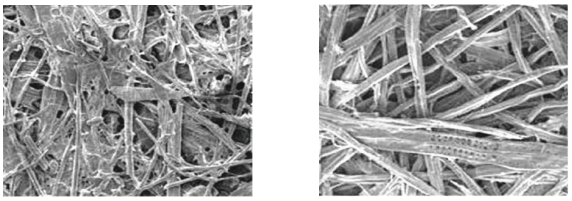

(a) (b)

Fig. 1. Fibre image. (a) Short fiber. (b) Long fiber.

Currently, the long fiber content (LFC) is usually used as an important technological index for the measurement of the mean of fiber length [10], [11]. In fact, merely by displaying the mean of the fiber length is not enough to describe the stochastic distribution characteristics. Using the mean of the fiber length as a controlled target in the refining process often causes the large fluctuations in the operating situations, it will seriously affects the stability of pulp quality. Existing researches have concluded that the pulp quality mainly depends on the shape of fiber length distribution (FLD) [6], [8], [9]. Therefore, the shape of FLD acts as a critical technological index in measuring the pulp quality in the refining process.

Over the past few decades, although academic and industrial researchers have proposed a series of control methods for the refining process [10]−[12], there are no research reports on the control of the refining process utilizing the shape of output FLD as a controlled target, this is mainly because the probability density function (PDF) shaping of output FLD exhibits strong non–Gaussian distribution characteristics, and the conventional control methods for the mean and variance of the fiber length are insufficient to control the PDF shaping

Manuscript received July 5, 2018; revised September 14, 2018; accepted October 14, 2018. This work was supported by the National Natural Science Foundation of China under Grants 61473064, 61333007, 61790572 and 61621004, by the Research Funds for the Central Universities under Grant N160805001 and Grant N160801001, and this work was also supported by the State (Beijing) Key Laboratory of Process Automation in Mining & Metallurgy (BGRIMM-KZSKL-2017-04).*(Corresponding author: Ping Zhou.)*

M. J. Li, P. Zhou and T. Y. Chai are with the State Key Laboratory of Synthetical Automation for Process Industries, Northeastern University, Shenyang 110819, China (e-mail: limingj88@126.com; zhouping@mail.neu.edu.cn; tychai@mail.neu.edu.cn).

H. Wang is with Pacific Northwest National Laboratory, Richland, WA 99352 USA (e-mail: hong.wang@pnnl.gov).

0278-0046 (c) 2018 IEEE. Personal use is permitted, but republication/redistribution requires IEEE permission. See http://www.ieee.org/publications_standards/publications/rights/index.html for more information.

This article has been accepted for publication in a future issue of this journal, but has not been fully edited. Content may change prior to final publication. Citation information: DOI 10.1109/TIE.2018.2879293, IEEE Transactions on Industrial Electronics

of output FLD effectively.

For the bounded dynamic stochastic systems with the output random variables following non–Gaussian type, Wang proposed a stochastic distribution control (SDC) approach since the principal purpose is to design the controller to make the output PDF shaping track a desired PDF shaping [13]−[15], and the SDC approaches have been successfully applied to some complex industrial processes [16]−[24] so far. For the dynamic stochastic distribution systems, the output PDF model generally includes an approximate part of output PDF with space–domain and a dynamic part of weight vector with time–domain. In general, the neural networks (NNs), such as B–spline NN [14], [15], RBF NN [17], [21], are employed to approximate the output PDF, and the dynamic model of weight vector is established by using the least square estimation or subspace identification method [13], [16], [17]. It has been shown that the output PDF model mainly depends on the basis functions and the dynamic model of weight vector, where the basis functions are generally given in advance. However, as the complexity of the practical industrial processes increases, the precision of output PDF model is not high by using NN with given basis functions, which makes the closed–loop system difficult to achieve satisfactory control effects. In order to tackle this problem, an iterative learning control (ILC) based modeling and controller design approach was presented for output PDF shaping of the stochastic distribution systems in [16], [17]. In these approaches, the RBF basis functions are employed to replace the B–spline basis functions and the center and the width of basis functions are treated as tuning parameters of the ILC law. That is to say, when the parameters of RBF basis functions are updated by an ILC law, the new dynamic PDF model can be established. At the same time, on the basis of the reconstructed dynamic PDF model, the ILC approach is also utilized to improve the tracking performances of stochastic distribution systems. In general, the idea of the ILC not only provides a control method to improve the closed-loop tracking performances, but also serves as an effective way to enhance the dynamic model accuracy of stochastic distribution systems.

For the practical process parameter such as the PDF shaping of output FLD in the refining process, it is necessary to ensure that the output PDF has an explicit physical significance. In other words, the output PDF is not only nonnegative after the final batch, but also exhibits nonnegativity within each batch. On the other hand, the controller with the P–type ILC law only considers the convergence of the closed–loop system in [16], [17], and the convergence rate of output PDF also cannot be ignored to achieve fast tracking of the desired PDF shaping.

Concentrated on these practical challenges, this paper proposes a novel geometric analysis based double closed–loop ILC method for the PDF shaping of output FLD in the refining process. Firstly, in order to make the PDF shaping of output FLD in the whole batches have a clear physical significance, it needs to be guaranteed nonnegative within each batch. Hence, the square root PDF model of output FLD characterizing dynamics of the refining process is employed. Meanwhile, the center and width of RBF basis functions are used as tuning parameters of the ILC law and the state–space model of weight vector can be established by the subspace identification method. Secondly, in order to improve the convergence rate of closed–loop system, this paper combines the SDC approaches with the ILC method based on geometric analysis [25] to achieve fast tracking of the desired PDF. Lastly, the effectiveness of the proposed method is verified by simulations, and satisfactory experimental results are achieved on the real refining process in a large–scale paper mill.

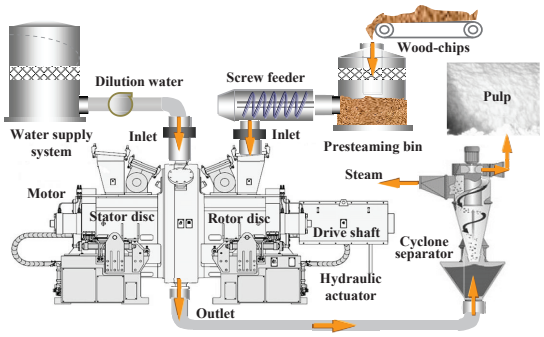

Fig. 2. Flowsheet of typical wood-chips refining process.

This paper is organized as follows. In Section II, the dynamic of the refining process and the double closed–loop ILC strategy are described, respectively. Then, the geometric analysis based double closed–loop ILC algorithm is described in Section III. Section IV studies the simulations and experiments in order to demonstrate the effectiveness of the proposed method. Finally, conclusions are given in Section V.

II. Process Description and Control Strategy

A. Refining Process Description

The flowsheet of typical wood–chips refining process is shown in Fig. 2. The refining process is the procedure of separating the fibers from the plant materials to obtain the pulps. It chiefly includes the feeding system, the dilution water supply system and the speed regulation system. When the refiner works, in order to obtain better fiber separation, the wood–chips are pretreated in the steamed warehouse at atmospheric pressure, impurities are removed through the washing system before transferred to the transfer screw feeder, and the wood–chips feeding rate are changed by adjusting the rotational speed of transfer screw feeder.

As the principal equipment in the refining process, the refiner is chiefly composed by the static disc, the rotating disc, the electric hydraulic servo device and the chief motor. When the pretreated wood–chips and the dilution water are injected into the refining zone, the plate gap can be adjusted by the electric–hydraulic servo device. In addition, the chief motor drives the rotating disc to work for converting the raw material of papermaking into individual fibers under the actions of mechanical friction, cutting, tearing and so on. Finally, the slurry is fed into the cyclone separator so as to obtain the fibers satisfying the requirements of papermaking process.

The primary manipulated variables in the refining process contain the rotating disc speed, the wood–chips feed rate, the plate gap and the dilution water flow rate. It is illustrated that

0278-0046 (c) 2018 IEEE. Personal use is permitted, but republication/redistribution requires IEEE permission. See http://www.ieee.org/publications_standards/publications/rights/index.html for more information.

This article has been accepted for publication in a future issue of this journal, but has not been fully edited. Content may change prior to final publication. Citation information: DOI 10.1109/TIE.2018.2879293, IEEE Transactions on Industrial Electronics

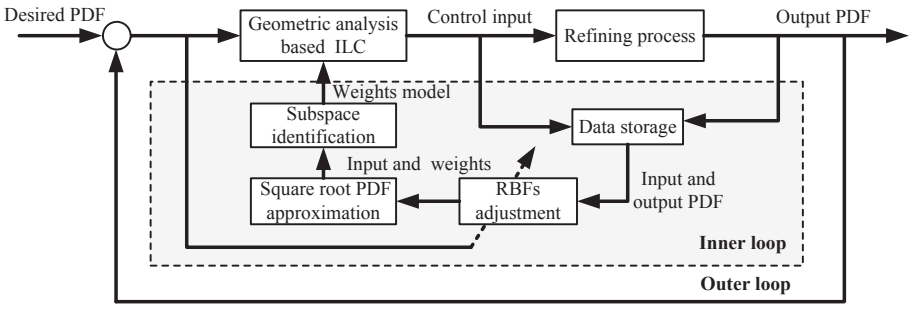

Fig. 3. Block diagram of the double closed-loop ILC structure.

the mean and variance of the fiber length are usually related to the dilution water flow rate and the plate gap [10], [11]. Additionally, according to the engineering experiences, the rotating disc speed is generally constant, when the production rate is given, the wood–chips feed rate is usually also constant. It can be seen that the control effects of the dilution water flow rate and the plate gap directly affect the PDF shaping of output FLD and play a key role in the refining process. Consequently, the plate gap and the dilution water flow rate are generally taken as the pivotal input variables that influence the PDF shaping of output FLD.

B. Double Closed-loop ILC Strategy

In this paper, a geometric analysis based ILC strategy with a double closed–loop structure is employed for the PDF shaping of output FLD in the refining process. The main design procedures of the double closed–loop ILC structure shown in Fig. 3 mainly include the ILC method based on geometric analysis in the outer loop, the dynamic PDF modeling by the subspace identification method and the parameters tuning of RBF basis functions between two adjacent batches by an ILC law in the inner loop. The detailed procedures are summarized as follows.

1) Select a set of initial RBF basis functions, then estimate the weight vector corresponding to the PDF of output FLD.
2) Multiply the estimated weight vector by the corresponding RBF basis functions to obtain the PDF of output FLD in the inner loop, and then calculate the approximation error.
3) The weight vector is calculated when the RBF basis functions are updated by using an ILC law, and then utilize the subspace identification method to construct the state–space model of weight vector.
4) The state–space model of weight vector is controlled in the outer loop by the ILC method based on geometric analysis and the input and output data are stored.
5) If the PDF tracking performance index meets the requirements, the iteration learning process is terminated, with the corresponding control input becoming the optimal control input. Otherwise, return to Step 1).

Remark 1: It is noted that the control horizon is divided into a number of batches with fixed RBF basis functions within each batch. Moreover, the dynamic output PDF model using the subspace identification method is utilized within the next batch of control. And the parameters of RBF basis functions are tuned by using the ILC law based on the stored data of output PDF and control input from the previous batches.

III. Geometric Analysis Based Double Closed-loop ILC Algorithm

A. PDF Model of Output FLD

For the dynamic stochastic system, denote the fiber length $y \in [a,\ \zeta]$ as the uniformly bounded and continuous random variable and assume that the fiber length y represents the output of the refining process by the control input u_k. Let $u_k \in \mathbb{R}^m$ be the control input that affects the distribution shape of the fiber length y. At each sample time k, the fiber length y can be characterized by its PDF $\gamma(y, u_k)$, which is defined as

$$P(a < y < \zeta, u_k) = \int_a^{\zeta} \gamma(y, u_k)\mathrm{d}y \tag{1}$$

where $P(a < y < \zeta, u_k)$ stands for the probability of the fiber length y within the interval $[a,\ \zeta]$ when the refining process affected by the control input u_k. This also means that the PDF $\gamma(y, u_k)$ of the fiber length y is affected by the control input u_k. Assuming that the bounded interval $[a,\ b]$ is known, and $\gamma(y, u_k)$ is continuous and bounded, to assure the nonnegativity of output PDF at the same time, it generally adopts the following square root PDF of output FLD, which can be approximated by

$$\sqrt{\gamma(y, u_k)} = \sum_{l=1}^{n} R_l(y)\omega_{l,k}(u_k) + e_0(y) \tag{2}$$

where $\omega_{l,k}(u_k)$ is the weight of the lth basis function $R_l(y)$, and $e_0(y)$ represents the approximation error. In this paper, the basis function is represented by the truncated Gaussian-type function of RBF NN in the following

$$R_l(y) = \exp\Big(\frac{(y-\mu_l)^2}{\sigma_l^2}\Big),\ l = 1,\ 2,\ \cdots,\ n. \tag{3}$$

where μ_l and σ_l are the center and width of the lth RBF basis function. Furthermore, the output PDF $\gamma(y, u_k)$ should satisfy that the integral in the bounded interval $[a,\ b]$ equals 1, namely $\int_a^b \gamma(y, u_k)\mathrm{d}y = 1$. To simplify Eq. (2), it is assumed that $e_0(y) \approx 0$, and Eq. (2) can be rewritten as follows

$$\sqrt{\gamma(y, u_k)} = C_0(y)V_k + R_n(y)\omega_{n,k} \tag{4}$$

0278-0046 (c) 2018 IEEE. Personal use is permitted, but republication/redistribution requires IEEE permission. See http://www.ieee.org/publications_standards/publications/rights/index.html for more information.

This article has been accepted for publication in a future issue of this journal, but has not been fully edited. Content may change prior to final publication. Citation information: DOI 10.1109/TIE.2018.2879293, IEEE Transactions on Industrial Electronics

where $C_0(y) = \left[R_1(y), R_2(y), \cdots, R_{n-1}(y)\right]$, $V_k = \left[\omega_{1,k}(u_k), \omega_{2,k}(u_k), \cdots, \omega_{n-1,k}(u_k)\right]^{\mathrm{T}}$. By squaring both sides of Eq. (2) and integrating on the definition domain, the nth weight $\omega_{n,k}$ can be obtained as follows [13], [19]

$$\omega_{n,k} = \frac{\sqrt{\Sigma_2 - V_k^{\mathrm{T}}(\Sigma_2\Sigma_0 - \Sigma_1^{\mathrm{T}}\Sigma_1)V_k} - \Sigma_1 V_k}{\Sigma_2} \tag{5}$$

where $\Sigma_0 = \int_a^b C_0^{\mathrm{T}}(y)C_0(y)\mathrm{d}y$, $\Sigma_1 = \int_a^b C_0(y)R_n(y)\mathrm{d}y$ and $\Sigma_2 = \int_a^b R_n^2(y)\mathrm{d}y$. It can be seen from Eq. (5) that if the nonlinear function $\omega_{n,k}$ exists, the following constraint condition is satisfied

$$V_k^{\mathrm{T}}\Sigma_2^{-1}(\Sigma_2\Sigma_0 - \Sigma_1^{\mathrm{T}}\Sigma_1)V_k \leq 1 \tag{6}$$

the inequality (6) can be regarded as the constraint condition that the weight vector needs to satisfy. As it can be seen from Eq. (4) that only the first $n-1$ weights in the n weights are independent.

Moreover, when the matrix $\begin{bmatrix}\Sigma_0 & \Sigma_1^{\mathrm{T}} \\ \Sigma_1 & \Sigma_2\end{bmatrix}$ is nonsingular, the inverse matrix always exists. Hence the weight vector can be calculated by using the following operation [13] based on the measured output PDF

$$\begin{bmatrix} V_k \\ \omega_{n,k}\end{bmatrix} = \begin{bmatrix}\Sigma_0 & \Sigma_1^{\mathrm{T}} \\ \Sigma_1 & \Sigma_2\end{bmatrix}^{-1}\begin{bmatrix}\int_a^b C_0^{\mathrm{T}}(y)\sqrt{\gamma(y,u_k)}\mathrm{d}y \\ \int_a^b R_n(y)\sqrt{\gamma(y,u_k)}\mathrm{d}y\end{bmatrix} \tag{7}$$

Eq. (7) reveals relationships between the weight vector and the output PDF. What can be seen is that when the RBF basis functions and the output PDF are known beforehand at any sampling time, the weight vector is readily available and the dynamic model of weight vector also can be established easily by the subspace identification method [26]. Consequently, the square root PDF model of output FLD characterizing the dynamic of the refining process can be expressed as follows

$$\begin{cases} x_{k+1} = Ax_k + Bu_k \\ V_k = Cx_k + Du_k \\ \sqrt{\gamma(y,u_k)} = C_0(y)V_k + R_n(y)\omega_{n,k}\end{cases} \tag{8}$$

where A, B, C, D denote state–space matrices, respectively, x_k and V_k denote the state variables and the weight vector, respectively, u_k represents the control input. It can clearly make out the dynamic relationship between the input variables and the PDF of output FLD, where the RBF basis functions and the weight vector collectively determine the PDF shaping of output FLD.

Remark 2: In order to make the PDF shaping of output FLD within all batches in the progress of modeling and control have a clear physical significance, it needs to be nonnegative within each batch. Hence, the square root PDF model of output FLD is employed in this paper.

Remark 3: As the major parameters of RBF basis functions, the center and width determine the accuracy of the output PDF model. However, if the center and width are not selected properly, the approximation results will be inaccurate or even impossible, which will cause large approximation errors along with affecting the model precision and the closed-loop performance directly.

B. Adjustment Algorithm in the Inner Loop–ILC Based RBF Basis Functions Tuning

The center and width of each RBF basis function can be adjusted by using an ILC law, so that the PDF error between the measured PDF and the approximate PDF is minimized. Suppose the measured PDF of all K times are expressed as a vector.

$$g(y) = \left[g_1(y), g_2(y), \cdots, g_K(y)\right] \tag{9}$$

The initial weight vector corresponding to the actual output PDF can be obtained through Eq. (7) when the initial center and width of RBF basis functions are given. The initial weight vector is then multiplied by the initial RBF basis functions, and the approximate PDF can be obtained. The center and width are adjusted according to the approximation error of the previous iteration. Suppose the approximation PDF after the ith batch is

$$\gamma_i(y) = \left[\gamma_{i,1}(y), \gamma_{i,2}(y), \cdots, \gamma_{i,K}(y)\right] \tag{10}$$

With the purpose of evaluating the approximation performances, the following quadratic performance indicator $J_{i,m}$ is employed to represent the PDF error between the measured PDF and the approximate PDF at the mth sampling point after the ith batch

$$J_{i,m} = \int_a^b \left(\sqrt{\gamma_{i,m}(y)} - \sqrt{g_m(y)}\right)^2 \mathrm{d}y \tag{11}$$

where $g_m(y)$ denotes the mth measured PDF sampling point. $\gamma_{i,m}(y)$ denotes the mth approximated PDF after the ith iteration.

The performance index vector within the ith iteration is $E_i = \left[J_{i,1}, J_{i,2}, \cdots, J_{i,K}\right]^{\mathrm{T}}$, and then the total modeling error after the ith iteration is expressed as $\overline{J}_{i,m} = \sum_{m=1}^{K} J_{i,m}$. Furthermore, the following ILC law is used for the tuning of the RBF basis functions between the $(i+1)$th and the ith batch, which can be expressed as follows

$$\begin{cases}\mu_{l,i+1} = \mu_{l,i} + \alpha_\mu E_i \\ \sigma_{l,i+1} = \sigma_{l,i} + \beta_\sigma E_i\end{cases} \tag{12}$$

where the learning rate α_μ and β_σ of the center and width are defined as follows

$$\begin{cases}\alpha_\mu = \zeta_\mu\left[\lambda_1,\ \lambda_2,\ \cdots,\ \lambda_K\right] \\ \beta_\sigma = \zeta_\sigma\left[\lambda_1',\ \lambda_2',\ \cdots,\ \lambda_K'\right]\end{cases}$$

in which ζ_μ and ζ_σ are respectively deterministic learning rate, the weight coefficient λ_1, λ_2, $\cdots$, λ_K and λ_1', λ_2', $\cdots$, λ_K' are defined as constants.

C. Control Algorithm in the Outer Loop–Geometric Analysis Based ILC of PDF Shaping of Output FLD

Consider the iterations of the double closed-loop structure, adding the iteration period i to the dynamic square root PDF model of output FLD shown in Eq. (8) leads to the following

$$\begin{cases} x_{i,k+1} = Ax_{i,k} + Bu_{i,k} \\ V_{i,k} = Cx_{i,k} + Du_{i,k} \\ \sqrt{\gamma(y,u_{i,k})} = C_0(y)V_{i,k} + R_n(y)\omega_{n,i,k}\end{cases} \tag{13}$$

0278-0046 (c) 2018 IEEE. Personal use is permitted, but republication/redistribution requires IEEE permission. See http://www.ieee.org/publications_standards/publications/rights/index.html for more information.

This article has been accepted for publication in a future issue of this journal, but has not been fully edited. Content may change prior to final publication. Citation information: DOI 10.1109/TIE.2018.2879293, IEEE Transactions on Industrial Electronics

where i indicates the ith iteration, and k represents the kth sample time within each batch.

Remark 4: In this paper, the square root PDF model is employed to guarantee the output PDF nonnegative within each batch, which not only requires the first $n-1$ weights to be nonnegative [13], [18], [19], but also needs the nth weight exists, that is, the first $n-1$ weights satisfy the constraint condition shown in Eq. (6).

For the traditional ILC algorithm, the main purpose is to make the actual weights track the desired weights, it adopts the following ILC algorithm to seek the optimal control input.

$$\begin{cases} u_{i+1,k} = u_{i,k} + Le_{i,k} \\ e_{i,k} = V_{i,k} - V_d, \ i = 1, \ 2, \ 3, \cdots \end{cases} \tag{14}$$

where $V_{i,k}$ represents the weight vector, V_d is the desired weight vector and L is the learning gain matrix remaining to be decided.

Remark 5: The traditional P–type ILC algorithm shown in Eq. (14) usually shows slow convergence rate, in order to improve the convergence rate of the closed-loop system, it is very necessary to seek a fast ILC algorithm in the outer loop. Therefore, it is motivated by an ILC algorithm based on geometric analysis in [25] whose main purpose is to achieve fast convergence rate.

Assume the desired weight vector is V_d, because of the refining process uncertainties, it is difficult to find the ideal control input u_d to produce its corresponding weight vector V_d. The conventional approach used is to seek the control input sequences $\{u_{i,k}\}$ through multiple iterative learning so that $u_{i,k}$ are constantly adjusted and eventually infinitely close to or equal to the ideal control input u_d. Denote $\hat{u}_{i,k} = u_{i,k} - u_d$, then Eq. (14) can be rewritten as

$$\hat{u}_{i+1,k} = \hat{u}_{i,k} + Le_{i,k} \tag{15}$$

To achieve $\hat{u}_{i,k} = u_{i,k} - u_d \to 0$, it only needs $\|\hat{u}_{i,k}\| \to 0$, namely, assuring $\|\hat{u}_{i,k}\|$ monotonically decreases in the determined algorithm of Eq. (15), and then it is easy to obtain the geometrical relation as shown in Fig. 4(a).

It requires looking for readjustment method of $\|\hat{u}_{i,k}\|$ on the basis of the analysis displayed in Fig. 4(a) in order to improve the convergence rate. In Fig. 4(b), the vertical line of $\|\hat{u}_{i,k}\|$ crossing the terminal point of $\|\hat{u}_{i,k}\|$ intersects $\|\hat{u}_{i+1,k}\|$ at point c, then it satisfies $\| \overrightarrow{oc} \| \leq \|\hat{u}_{i+1,k}\|$ and $\| \overrightarrow{oc} \| > \|\hat{u}_{i,k}\|$. And then pass point a to make vector $\overrightarrow{ad}$ intersect $\overrightarrow{ob}$ at point d as shown in Fig. 4(c), it can be observed that only when $\beta \leq 90^{\circ}$, can $\| \overrightarrow{od} \|$ be less than $\|\hat{u}_{i,k}\|$.

Denoting $\overrightarrow{ad} = \hat{e}_{i,k}$ and taking $\hat{u}^*_{i+1,k} = \overrightarrow{od}$ to adjust $\hat{u}_{i+1,k}$, then the corresponding control algorithm equals as follows.

$$\hat{u}^*_{i+1,k} = \hat{u}_{i,k} + L\hat{e}_{i,k} \tag{16}$$

It turns out from Eq. (16) that the condition $\| \hat{u}^*_{i+1,k} \| \leq \| \hat{u}_{i,k} \|$ is satisfied. Hence the issue comes to how to ascertain $\hat{e}_{i,k}$ so that it comes to $\beta \leq 90^{\circ}$. As is shown in Fig. 4(c), when we select the vector conforming with $\overrightarrow{oc} \perp Le_{i-1,k}$, if it meets $\alpha > 0$, then we get $\beta \leq 90^{\circ}$, that is to say, it works

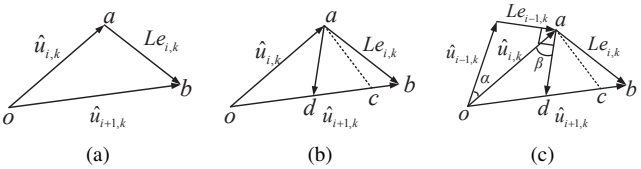

Fig. 4. Geometric analysis diagram.

as long as the choice $\hat{e}_{i,k} \perp Le_{i-1,k}$ is made. Obviously, it can be deduced that

$$\hat{e}_{i,k} = Le_{i,k} - \frac{(Le_{i-1,k})^{\mathrm{T}} Le_{i,k}}{\|Le_{i-1,k}\|^2} Le_{i-1,k} \tag{17}$$

which is perpendicular to $Le_{i-1,k}$.

An adaptive factor η is introduced into Eq. (17) so that the improved ILC algorithm can be more flexible and is associated with the traditional ILC algorithm as shown in Eq. (14), where the improved ILC algorithm is represented as follows

$$u_{i+1,k} = u_{i,k} + L\Big(e_{i,k} - \eta \frac{(Le_{i-1,k})^{\mathrm{T}} Le_{i,k}}{\|Le_{i-1,k}\|^2} e_{i-1,k}\Big) \tag{18}$$

With the decrease of the parameter η, the control performance in Eq. (18) is gradually weakened, because its corresponding length of $\|\hat{u}_{i+1,k}\|$ is gradually increasing, and the corresponding algorithm performs the worst if $\eta = 0$. In another case, that is, in the case of Eq. (18) for $\| \hat{u}_{i+1,k} \| < \| \hat{u}_{i,k} \|$, the performance of the algorithm shown in Eq. (18) coincides with the case of $\| \hat{u}_{i+1,k} \| \geq \| \hat{u}_{i,k} \|$ corresponding to Fig. 4(c). On the contrary, it gets worse with the increase of η, and when $\eta = 1$ it displays the worst performance.

When the adaptive factor $\eta = 0$, Eq. (18) becomes the conventional ILC algorithm shown in Eq. (14), while if $\eta = 1$, Eq. (18) becomes the generalized form of the ILC algorithm shown in Eq. (18). As shown in Fig. 4(c), the ILC algorithm in Eq. (18) performs the best, whose corresponding length of $\|\hat{u}_{i,k}\|$ is the shortest.

From the above analysis, the adaptive factor η should be adjustable along with the advances of the batches so as to make the algorithm in Eq.(18) optimal. Namely, the adaptive factor should increase with the increase of the error and decrease with the reduction of the error in the iterative process. Hence, the adaptive factor η is chosen as follows

$$\eta = \alpha\big(1 - \exp(-\beta \|e_{i,k}\|)\big) \tag{19}$$

The aforementioned $\alpha \in (0,1)$, $\beta \in (0, +\infty)$ are both adjustable parameters that determine how the adaptive factor η vary with the error. In summary, the above ILC algorithm with an adaptive factor can be obtained in the following.

$$\begin{aligned} u_{i+1,k} = u_{i,k} + Le_{i,k} - \alpha L\big(1 - \exp(-\beta \|e_{i,k}\|)\big) \\ \times \frac{(Le_{i-1,k})^{\mathrm{T}} Le_{i,k}}{\|Le_{i-1,k}\|^2} e_{i-1,k} \end{aligned} \tag{20}$$

where the control input $u_{i,k} = [u_{1,i,k}, \ u_{2,i,k}]^{\mathrm{T}}$ is a two-dimensional vector, $u_{1,i,k}$ and $u_{2,i,k}$ represent the dilution water flow rate and the plate gap, respectively.

0278-0046 (c) 2018 IEEE. Personal use is permitted, but republication/redistribution requires IEEE permission. See http://www.ieee.org/publications_standards/publications/rights/index.html for more information.

This article has been accepted for publication in a future issue of this journal, but has not been fully edited. Content may change prior to final publication. Citation information: DOI 10.1109/TIE.2018.2879293, IEEE Transactions on Industrial Electronics

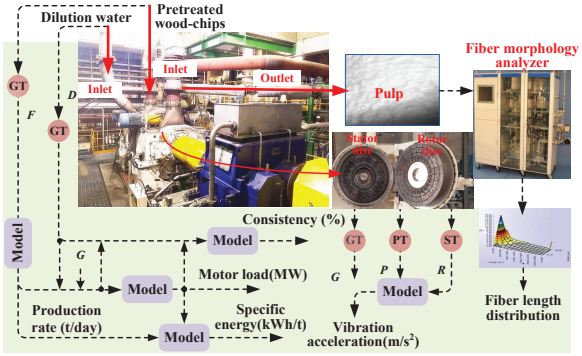

Fig. 5. Refining process in the industrial field.

Remark 6: For the square root PDF model of output FLD characterizing the refining process with non–Gaussian stochastic distribution dynamics shown in Eq. (13), the proposed method can not only guarantee that the output PDF is non negative within each iteration, but also can effectively improve the convergence rate and tracking performances of the closed-loop system.

Remark 7: For an iterative learning algorithm, convergence is an important prerequisite for ensuring the practicability of the algorithm. In this paper, the convergence conditions and analysis of the proposed algorithm are similar to those in [16] and [25], and it is not restated here for saving space.

IV. Simulations and Experiments

To demonstrate the effectiveness and practicability of the proposed method, the simulations on the basis of the real industrial data from a paper mill in southern China have been carried out in the refining process as shown in Fig. 5 and the principal technical parameters of the key equipment are shown in Table I.

According to the mechanism analysis of the refining process, the key variables affecting the output PDF shaping of FLD mainly include the wood–chips feed rate (kg/h), the dilution water flow rate (l/min), the plate gap (mm), the hydraulic closing pressure (kPa), the rotor disc speed (r/min), the transfer screw speed (r/min), the motor load (MW), the refiner vibration acceleration ($\mathrm{m/s^2}$), the production rate (t/day), the pulp consistency (%) and the specific energy (kWh/t). Among them, the first five variables can achieve online measurement easily. Table II lists the directly measured variables and their instrumentations. These directly measured variables are used to calculate other variables that cannot be measured online according to their empirical models.

In the practical refining process, the data of the above-mentioned variables are recorded online in real time and simultaneously the PDF data of output FLD is collected by the Kajaani fiber and pulp analyzers every 10 minutes. Moreover, when the production rate is fixed, the transfer screw speed and wood–chips feed rate are usually constant and the rotational disc speed is generally also constant. Consequently, we take the dilution water flow rate and the plate gap as the chief input variables influencing the PDF shaping of output FLD.

TABLE I
Principal Technical Parameters of Equipments

Equipments	Principal technical parameters
Double disc refiner	Disc diameter: ϕ 1980mm; Maximal motor power: 40MW; Spindle speed: 6000r/min; Maximal production capacity: 800 tonne/day.
Electrical-hydraulic servo system	Operating pressure: 10Mpa; Hydraulic cylinder diameter: 50mm; Piston rod diameter: 30mm; Servo valve rated flow: 2×10^{-4} $\mathrm{m^3/s}$; Hydraulic oil concentration: ρ=880 $\mathrm{m^3/kg}$.
Kajaani fiber and pulp analyzers	Testing range: 0.05mm−2.30 mm, Testing time: 240s.
LS type screw feeder	Screw rotation speed: 20−500rpm; screw conveyor length: 1m; Spiral diameter: 150mm; Motor power: 20kW
Water supply pump	Motor power: 4kW

TABLE II
Directly Detecting Variables and Their Instructions

Variables (symbol)	Unit	Instrumentation (symbol)
Wood-chips feed rate(F)	kg/h	Honeywell ultraprecise turbine flowmeter (FT)
Dilution water flow rate (D)	l/min	Honeywell ultraprecise turbine flowmeter (FT)
Plate gap (G)	mm	Honeywell Noncontact displacement sensor (GT)
Hydraulic closing pressure (P)	Kpa	KISTLER pressure transducers (PT)
Rotating disc speed (R)	r/min	Photoelectric speed measuring sensor (ST)

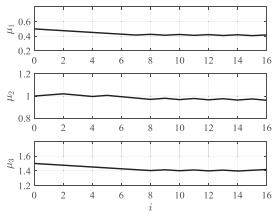

Fig. 6. Center variation trend.

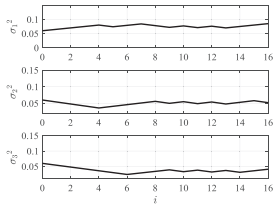

Fig. 7. Width variation trend.

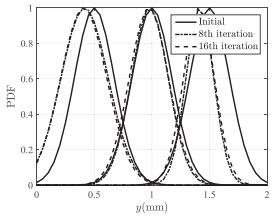

Fig. 8. Position variation trend.

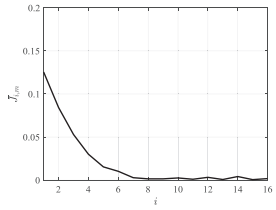

Fig. 9. Performance index of the modeling error.

A. Industrial Data Based Simulations

1) PDF Model of Output FLD Establishment: The collected 100 groups of industrial data are utilized for simulations, which include the PDF of output FLD, the dilution water flow rate and the plate gap. In order to establish the square root PDF model of output FLD in the refining process, the tuning method of RBF basis functions that uses the ILC law and the subspace identification method for constructing the state-space model of weight vector are adopted, respectively. And the learning rates of center and width are set as $\zeta_\mu = 0.02$, $\zeta_\sigma = 0.01$, the initial center and width of RBF basis functions

0278-0046 (c) 2018 IEEE. Personal use is permitted, but republication/redistribution requires IEEE permission. See http://www.ieee.org/publications_standards/publications/rights/index.html for more information.

This article has been accepted for publication in a future issue of this journal, but has not been fully edited. Content may change prior to final publication. Citation information: DOI 10.1109/TIE.2018.2879293, IEEE Transactions on Industrial Electronics

are chosen as $\mu_1 = 0.5$, $\mu_2 = 1.0$, $\mu_3 = 1.5$, $\sigma_1^2 = \sigma_2^2 = \sigma_3^2 = 0.06$. After the 16th iteration, the center and width of RBF basis functions are obtained as $\mu_1 = 0.416$, $\mu_2 = 0.958$, $\mu_3 = 1.402$, $\sigma_1^2 = 0.076$, $\sigma_2^2 = 0.056$, $\sigma_3^2 = 0.044$.

The varying trends of center and width with iterations is displayed in Figs. 6 and 7. What can be seen from Figs. 6 and 7 is that the center and width tend to be stable after the 16th iteration. Furthermore, the position variation trend of RBF basis function is displayed in Fig. 8 after the 8th batch and the 16th batch, from which it can be seen that as iterations increase, the position of the center and width gradually shift to the ideal position. Meanwhile, it is obviously observed from Fig. 9 that the performance index of the total modeling error decreases monotonically along with batches and it changes slightly after the 8th batch.

When the RBF basis functions tuning is accomplished, the estimation of the weight vector can be realized effectively by using Eq. (7) for the measured PDF of output FLD. Moreover, since the output PDF satisfies the natural constraint condition that the integral of PDF in the bounded interval $[a, b]$ equals 1, the first two weights are independent from each other and the third weight is nonlinearly related to the first two weights.

After the calculation of weight vector, the state–space model order is determined based on the singular value decomposition technique, and the subspace identification method is employed to establish the state-space model of the weight vector. In this paper, the model order is selected as 2, and the state-space model of weight vector is obtained as follows

$$A = \begin{bmatrix} 0.778 & -0.005 \\ -0.20 & -0.01 \end{bmatrix},\ B = \begin{bmatrix} -0.066 & -0.113 \\ -0.015 & -0.173 \end{bmatrix},$$
$$C = \begin{bmatrix} -0.704 & 0.013 \\ 0.136 & -0.167 \end{bmatrix},\ D = 0. \tag{21}$$

2) Geometric Analysis Based ILC Effects: Given to the desired PDF shaping of output FLD, the desired weight vector can be estimated using Eq. (7), in which only the first two elements are fetched. In order to demonstrate the superiority of the proposed method, we adopt the proposed method comparing with the conventional ILC method in Eq. (14). Here we choose $\alpha = 0.75$, $\beta = 0.85$, $L = \begin{bmatrix} 1 & 1 \\ 0 & 1 \end{bmatrix}$, $V_d = \begin{bmatrix} 1.55 & 0.562 \end{bmatrix}^{\mathrm{T}}$. The initial weight vector is set $V_0 = \begin{bmatrix} 1.65 & 0.15 \end{bmatrix}^{\mathrm{T}}$ within each batch. Suppose that the number of sampling points within each batch is 30, that is $k = 1, 2, \cdots, 30$, then the proposed method in the outer loop can be expressed as

$$u_{i+1,k} = u_{i,k} + Le_{i,k} - 0.75L\big(1 - \exp(-0.85\|e_{i,k}\|)\big) \times \frac{(Le_{i-1,k})^{\mathrm{T}} Le_{i,k}}{\|Le_{i-1,k}\|^2} e_{i-1,k} \tag{22}$$

Under the traditional ILC method in Eq. (14) and the proposed method, the convergence of PDF of output FLD after the 16th batch is shown in Fig. 10. The PDF shaping of output FLD can achieve satisfactory control results by the proposed method after the 7th batch, while there exists relatively large error between the PDF of output PDF and the desired PDF by the traditional ILC method after the 16th batch. This

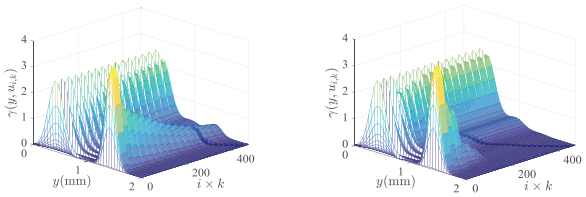

Fig. 10. Convergence of the PDF of output FLD with two methods in all batches. (a) Conventional ILC method. (b) Geometric analysis based ILC method.

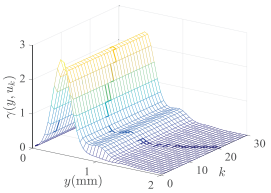

Fig. 11. Output PDF within the final batch.

comparison has verified the fact that the convergence rate of the closed–loop system by using the proposed method is much faster than that of the traditional ILC method. Moreover, the resulting PDF shaping of output FLD within the final batch is displayed in Fig. 11. It is intuitively seen that the PDF shaping of output PDF approaches the desired PDF gradually and finally gets to the desired PDF shaping within the final batch. Therefore, the proposed method can not only guarantee the stability of the closed–loop system, but also can effectively improve the convergence rate of output PDF.

Remark 8: Through the analysis of large number of industrial data after the engineer testing, the desired PDF shaping of output FLD can be determined combining with the relevant expert knowledge, and then the corresponding desired weight vector can be estimated using Eq. (7).

B. Experiments

In order to further verify the practicability and superiority of the proposed method, the proposed method is tested on this real wood–chips refining process. In the past, the long fiber content (LFC) is regarded as a technological index of pulp quality for measuring the traditional mean of fiber length, which usually needs to ensure that the LFC is regulated between 53% and 57%, with the same sampling period of PDF of output FLD. Currently, it mainly relies on the manual control method to adjust the plate gap and the dilution water flow rate to achieve the LFC regulation, whose control results are shown in Fig. 12. It can be seen that the manual control method for LFC not only makes the pulp quality difficult to control within the range of technological requirements, but also seriously affects the stability of the refining process since the repeated adjustments of the plate gap and the dilution water flow rate.

In addition, the control results within 4 hours using the proposed method are shown in Fig. 13. At the beginning of the data test, it is obviously seen from Fig. 13 that there

0278-0046 (c) 2018 IEEE. Personal use is permitted, but republication/redistribution requires IEEE permission. See http://www.ieee.org/publications_standards/publications/rights/index.html for more information.

This article has been accepted for publication in a future issue of this journal, but has not been fully edited. Content may change prior to final publication. Citation information: DOI 10.1109/TIE.2018.2879293, IEEE Transactions on Industrial Electronics

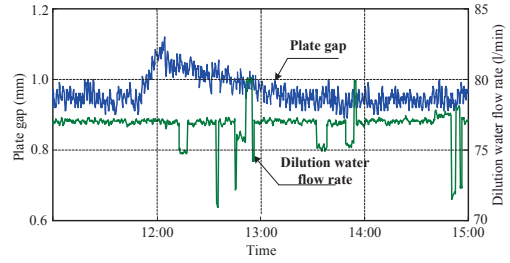

(a)

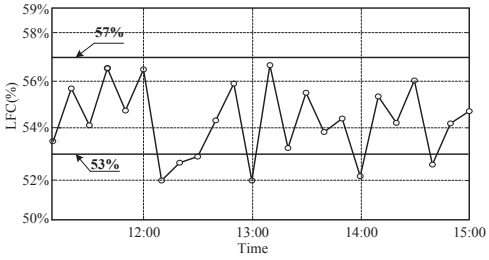

(b)

Fig. 12. Control effects when using manual control of LFC. (a) Trends of plate gap (mm) and dilution water flow rate (l/min). (b) Trends of long fiber content (LFC).

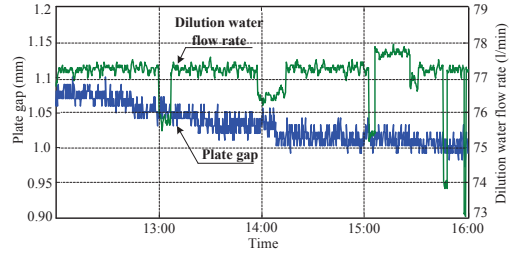

(a)

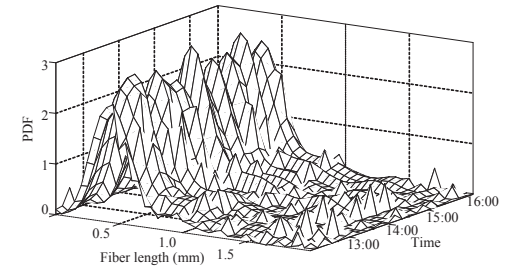

(b)

Fig. 13. Control effects when using the proposed method. (a) Trends of plate gap (mm) and dilution water flow rate (l/min). (b)PDF shaping of output FLD.

exist certain fluctuations in the PDF of output FLD. However, the plate gap and the dilution water flow rate gradually turn stable and the PDF shaping of output FLD is getting closer to the desired PDF shaping. This is because the tracking performance of the closed–loop system is improved due to the continuous iterative updates. In general, when compared with the manual control method for LFC, the proposed method not only effectively improves the pulp quality, but also increases the stability of the closed–loop system.

V. Conclusions

In view of the issues of the control engineering in the current papermaking industry, in order to improve the pulp quality and to reduce the energy consumption, the optimal control of the refining process means the control of the final pulp quality. However, the traditional mean and variance of fiber length are difficult to be used as measures of pulp quality, this is mainly because the PDF shaping of output FLD shows strong non–Gaussian stochastic distribution characteristic. Therefore, the traditional control of the mean and variance of fiber length is difficult to control the PDF shaping of output FLD effectively.

In this paper, a geometric analysis based double closed–loop ILC method is proposed for the PDF shaping of output FLD in the refining process. In the proposed method, the square root PDF approximation is adopted based on the RBF NN so as to ensure that the output PDF is nonnegative. On the other hand, a geometric analysis based ILC strategy is utilized in order to improve the convergence rate of the closed–loop system, and the parameters of RBF basis functions between batches are tuned using an ILC law so that the output PDF gets closer to the desired PDF within the next batch. Both simulations and experiments results demonstrate that the proposed method can not only guarantee the closed–loop stability as well as accelerating the convergence rate of output PDF, but also improve the pulp quality and strengthen the stability of the refining process.

Acknowledgment

The authors would like to thank the editor, the associate editor, and the anonymous reviewers for their constructive comments which helped to improve the quality of this paper. They would also like to thank R. Z. Du for his suggestions which improved this paper.

References

[1] M. Elsinga, "TMP optimization using multivariate analysis," *IEEE Trans. Industry Appl.*, vol. 39, no. 3, pp. 893–898, May–Jun. 2003.

[2] A. Runkler, E. Gerstorfer, M. Schlangc, E. J. unnemannd, and J. Hollatz, "Modelling and optimization of a refining process for fiber board production," *Control Eng. Pract.*, vol. 11, pp. 1229–1241, Nov. 2003.

[3] P. Zhou, H. Wang, M. J. Li, Z. C. Zhao, and T. Y. Chai, "Data–driven ALS–SVR–ARMA2K modelling with AMPSO parameter optimization for a high consistency refining system in papermaking," *IET Control Theory Appl.*, vol. 10, no. 14, pp. 1620–1629, 2016.

[4] S. Andersson, C. Sandberg, and P. Engstrand, "Effect of long fiber concentration on low consistency refining of mechanical pulp," *Nordic Pulp Paper Res. J.*, vol. 27, no. 4, pp. 702–706, Jan. 2013.

[5] Q. X. Hou, L. H. Liu, W. Liu, Y. Wang, N. P. Xu, and Q. Liang, "Achieving refining energy savings and pulp properties for poplar chemithermo mechanical pulp improvement through optimized auto hydrolysis pretreatment," *Ind. Eng. Chem. Res.*, vol. 53, no. 45, pp. 17843–17848, 2014.

[6] P. Zhou, M. J. Li, D. W. Guo, H. Wang, and T. Y. Chai, "Modeling for output fiber length distribution of refining process using wavelet neural networks trained by NSGA–II and gradient based two–stage hybrid algorithm," *Neurocomputing*, vol. 238, no. C, pp. 24–32, May. 2017.

[7] P. Afshar, M. Brown, J. Maciejowski, and H. Wang, "Data–based robust multiobjective optimisation of interconnected processes: energy efficiency case study in papermaking," *IEEE Trans. Neural Netw.*, vol.22, no. 12, pp. 2324–2338, Dec. 2011.

[8] S. Gharehkhani, E. Sadeghinezhad, S. N. Kazi, H. Yarmanda, A. Badarudina, M. R. Safaei, and M. N. Zubira, "Basic effects of pulp refining on fiber properties–A review," *Carbohydrate Polym.*, vol. 115, no. 22, pp. 785–803, Jan. 2015.

0278-0046 (c) 2018 IEEE. Personal use is permitted, but republication/redistribution requires IEEE permission. See http://www.ieee.org/publications_standards/publications/rights/index.html for more information.

This article has been accepted for publication in a future issue of this journal, but has not been fully edited. Content may change prior to final publication. Citation information: DOI 10.1109/TIE.2018.2879293, IEEE Transactions on Industrial Electronics

[9] T. M. Lacerda, M. D. Zambon, and E. Frollini, "Effect of acid concentration and pulp properties on hydrolysis reactions of mercerized sisal," *Carbohydrate Polym.*, vol. 93, no. 1, pp. 347–356, Mar. 2013.

[10] E. Harinath, L. T. Biegler, and G. A. Dumont, "Control and optimization strategies for thermo–mechanical pulping processes: nonlinear model predictive control," *J. Process Control*, vol. 21, no. 4, pp. 519–528, Apr. 2011.

[11] E. Harinath, L. T. Biegler, and G. A. Dumont, "Predictive optimal control for thermo-mechanical pulping processes with multi-stage low consistency refining," *J. Process Control*, vol. 23, no. 7, pp. 1001–1011, Aug. 2013.

[12] M. Tervaskanto, E. Ikonen, and T. Ahvenlampi, "Refiner quality control in a CTMP plant," in *Proc. IEEE. Conf. Control and Automat.*, Christchurch, New Zealand, pp. 1266–1270, Dec. 2009.

[13] H. Wang, *Bounded Dynamic Stochastic systems: Modelling and Control.* London: Springer–Verlag Ltd, 2000.

[14] H. Wang, "Robust control of the output probability density functions for multivariable stochastic systems with guaranteed stability," *IEEE Trans. Automat. Control*, vol. 22, no. 12, pp. 2324–2338, Dec. 2011.

[15] H. Wang, "Minimum entropy control for non–Gaussian dynamic stochastic systems," *IEEE Trans. Automat. Control*, vol. 47, no. 2, pp. 398–403, Feb. 2002.

[16] H. Wang and P. Afshar, "ILC–based fixed–structure controller design for output PDF shaping in stochastic systems using LMI technique," *IEEE Trans. Automat. Control*, vol. 54, no. 4, pp. 760–773, Apr. 2009.

[17] J. L. Zhou, H. Yue, J. F. Zhang, and H. Wang, "Iterative learning double closed–loop structure for modeling and controller design of output stochastic distribution control systems," *IEEE Trans. Control Syst. Technol.*, vol. 22, no. 6, pp. 2261–2276, Nov. 2014.

[18] J. L. Zhou, X. Wang, J. F. Zhang, H. Wang, and G. H. Yang, "A new measure of uncertainty and the control loop performance assessment for output stochastic distribution systems," *IEEE Trans. Automat. Control*, vol. 60, no. 9, pp. 2524–2529, Sep. 2015.

[19] J. L. Zhou, G. T. Li ,and H. Wang, "Robust tracking controller design for non-Gaussian singular uncertainty stochastic distribution systems," *Automaica*, vol. 50, no. 4, pp. 1296–1303, Apr. 2014.

[20] J. F. Zhang, H. Yue, and J. L. Zhou, "Predictive PDF control in shaping of molecular weight distribution based on a new modeling algorithm," *J. Process Control*, vol. 30, pp. 80–89, Jun. 2015.

[21] A. P. Wang, P. Afshar, and H. Wang, "Complex stochastic system modeling and control via iterative machine learning," *Neurocomputing*, vol. 71, nos. 13–15, pp. 2685–2692, Aug. 2008.

[22] X. B. Sun, J. L. Ding, H. Wang, T. Y. Chai, and H. R. Dong, "Iterative learning based particle size distribution control in grinding process using output PDF method," *In Proc. Int. Conf. Control and Automat.*, Hangzhou, China, 2013, pp. 63–38.

[23] Y. W. Ren, A. P. Wang, and H. Wang, "Fault diagnosis and tolerant control for discrete stochastic distribution collaborative control systems," *IEEE Trans. Syst., Man, Cybern: Syst.*, vol. 45, no. 3, pp. 462–471, Mar. 2015.

[24] J. Y. Zhu, W. H. Gui, J. P. Liu, H. L. Xu, and C. H. Yang, "Combined fuzzy based feedforward and bubble size distribution based feedback control for reagent dosage in copper roughing process," *J. Process Control*, vol. 39, pp. 50–63, Mar. 2016.

[25] S. L. Xie, S. P. Tian, and Z. D. Xie, *Theory and Application of Iterative Learning Control.* Beijing: Science Press, 2005.

[26] P. V. Overchee and B. D. Moor, *Subspace Identification of Linear Systems: Theory–Implementation–Applications.* Dordrecht, Netherlands: Kluwer, 1996.

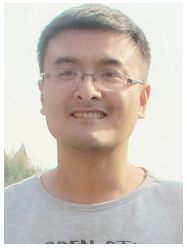

Mingjie Li received the M.S. degree in Control Theory and Control Engineering from Taiyuan University of Science and Technology, Taiyuan, China, in 2014. He is currently working toward the Ph.D. degree in the State Key Laboratory of Synthetical Automation for Process Industries, Northeastern University, Shenyang, China. His main research interests include modeling and control for complex industrial process.

Ping Zhou (M'12–SM'17) received the B.S., M.S., and Ph.D. degrees in control theory and engineering from Northeastern University, Shenyang, China, in 2003, 2006, and 2013, respectively.

He is currently a Professor with the State Key Laboratory of Synthetical Automation for Process Industries, Northeastern University. He has authored over 80 papers and one monograph in these research areas. His current research interests include the development of feedback control for optimal process operation, and data-driven modeling and control.

Dr. Zhou was a recipient of the Rockwell Automation Award for the Outstanding Application Paper with the Six World Congress on Intelligent Control and Automation, and the Keynote Paper Award for the Outstanding Application Paper with the 26th Chinese Process Control Conference.

Hong Wang (M'97–SM'02) received the B.S. degree from the Huainan University of Mining Engineering, Huainan, China, in 1982, and the M.S. and Ph.D. degrees from the Huazhong University of Science and Technology, Wuhan, China, in 1984 and 1987, respectively.

In 1992, he joined the University of Manchester Institute of Science and Technology, Manchester, U.K., where he was a Professor of process control between 2002 and 2016. He was a Research Fellow with Salford University, Salford, U.K., Brunel University, Uxbridge, U.K., and Southampton University, Southampton, U.K. Since 2016, he has been a Laboratory Fellow and Chief Scientist with Pacific Northwest National Laboratory, Richland, WA, USA. He has authored 200 papers and three books in these research areas. His current research interests include stochastic distribution control, fault detection and diagnosis, nonlinear control, and data-based modeling for complex systems.

Dr. Wang was an Associate Editor of the IEEE TRANSACTIONS ON AUTOMATIC CONTROL. He currently serves as an Associate Editor of the IEEE TRANSACTIONSON CONTROL SYSTEMS TECHNOLOGY and the IEEE TRANSACTIONS ON AUTOMATION SCIENCE AND ENGINEERING.

Tianyou Chai (M'07) received the Ph.D. degree in control theory and engineering from Northeastern University, Shenyang, China, in 1985.

He is currently the Founder and the Director of the Center of Automation, which became a National Engineering and Technology Research Center, Shenyang, China, in 1997. He has authored three monographs, more than 120 peer-reviewed international journal papers, and around 224 international conference papers. His current research interests include adaptive control, intelligent decoupling control, and the development of control technologies with applications to various industrial processes.

Dr. Chai received three prestigious awards of the National Science and Technology Progress: the 2002 Technological Science Progress Award from Ho Leung Ho Lee Foundation, the 2007 Industry Award for Excellence in Transitional Control Research from the IEEE Control Systems Society, and the 2010 Yang Jia-Chi Science and Technology Award from the Chinese Association of Automation. He is a member of the Chinese Academy of Engineering, an Academician of the International Eurasian Academy of Sciences, and a fellow of International Federation of Automatic Control. He is also a Distinguished Visiting Fellow with the Royal Academy of Engineering, U.K., and an Invitation Fellow of Japan Society for the Promotion of Science.

0278-0046 (c) 2018 IEEE. Personal use is permitted, but republication/redistribution requires IEEE permission. See http://www.ieee.org/publications_standards/publications/rights/index.html for more information.